scientific reports

Check for updates

OPEN

Calcium ions play a critical role in calcification of *Corynebacterium matruchotii*

Naoko Ohara[1], Midori Ogawa[2], Katsuki Takebe[3], Ikue Tosa[4,5], Serina Ono[1], Mitsumasa Saito[2] & Naoya Ohara[4,5,6]✉

Dental calculus is a hardened deposit composed of calcium phosphate precipitated within dental plaque. While the involvement of dental calculus in the progression of periodontal disease is well established, many aspects of its formation process remain poorly understood. In this study, we focused on *Corynebacterium matruchotii*, a key bacterium involved in dental calculus formation, and investigated the role of calcium ions in calcification, as well as the associated internal and external changes in the bacterium through long-term observation. In the absence of calcium ions, no intracellular calcification was observed, and the lipid bilayer with the formation of holes in bacterial body was evident. In contrast, in the presence of calcium ions, lipid bilayer remained intact, and intracellular needle- and plate- like crystals were formed. Furthermore, calcified *C. matruchotii* showed increased flocculation compared to non-calcified *C. matruchotii*. These results indicate that the influx of calcium ions is essential for intracellular calcification. Calcium ions entry appears to reinforce the integrity of the lipid bilayer, providing a stable intracellular environment conductive to calcification. Moreover, calcified *C. matruchotii* may contribute to the nucleation of dental calculus by forming aggregates composed of both bacterial components and calcified material.

Keywords Calcification, *Corynebacterium matruchotii*, Dental calculus, Calcium ions

Oral bacteria adhere to tooth surfaces via saliva-derived glycoproteins, leading to the formation of biofilms through bacterial growth and co-aggregation[1,2]. This biofilm, also known as dental plaque, is a major etiological factor in the development of dental caries and periodontal diseases such as periodontitis[3,4]. Dental calculus is a calcified form of dental plaque composed primarily of dead bacteria and calcium phosphate. It is typically classified into two types: supragingival and subgingival calculus[5].

The pathogenicity of dental calculus is not solely due to its physical presence. While it mechanically irritates gingival tissues and obstructs the flow of saliva and gingival crevicular fluid, its rough and porous surfaces also promote bacterial adherence and proliferation. Moreover, bacterial components embedded in the calculus are believed to contribute to persistent inflammation and disease progression[6–8]. Despite its pathological significance, dental calculus adheres tightly to tooth surfaces and cannot be removed by toothbrushing or chemical agents, requiring the use of specialized dental instruments[9]. Therefore, the removal of dental calculus is a central component in the treatment of periodontal disease, and understanding its formation is essential to elucidating the pathophysiology of periodontal diseases[10].

Corynebacterium matruchotii is a Gram-positive rod-shaped bacterium and one of the most abundant species in dental plaque[11]. It has been observed to interact with both *Streptococcus* and *Actinomyces*[12], forming the structural core of plaque. Moreover, *C. matruchotii* is known to undergo intracellular calcification and has been suggested to contribute to dental calculus formation, a pathogenic factor in oral diseases. Therefore, *in vitro* studies on *C. matruchotii* have conducted to analyze the process of dental calculus formation[13–16]. Similarly, *Escherichia coli* has been shown to form needle- and plate-like intracellular crystals containing calcium and phosphorus ions inside the bacterial body[17]. A prerequisite for such bacterial calcification is bacterial degeneration

[1]Department of Operative Dentistry, Faculty of Medicine, Dentistry and Pharmaceutical Sciences, Okayama University, Okayama, Japan. [2]Department of Microbiology, School of Medicine, University of Occupational and Environmental Health, Fukuoka, Japan. [3]Department of Dental Pharmacology, Faculty of Medicine, Dentistry and Pharmaceutical Sciences, Okayama University, Okayama, Japan. [4]Department of Oral Microbiology, Faculty of Medicine, Dentistry and Pharmaceutical Sciences, Okayama University, 2-5-1 Shikata-cho, Kita-ku, Okayama- city 700-8525, Okayama, Japan. [5]Advanced Research Center for Oral and Craniofacial Sciences, Dental School, Okayama University, Okayama, Japan. [6]Research Center for Intestinal Health Science, Okayama University, Okayama, Japan. ✉email: oharan@md.okayama-u.ac.jp

which may occur as a result of bacterial aging or exposure to external stressors[18,19]. In *E. coli*, extracellular phosphoproteins have been suggested as a potential source of phosphate of intracellular calcification, and silicon has been identified as a critical nucleation factor in *C. matruchotii*[20]. However, while the roles of phosphate and silicon have been explored, the direct contribution of calcium ions – the other major component of bacterial calcification – remains poorly understood.

In this study, we investigated the role of extracellular calcium ions in bacterial calcification by observing the long-term process of intracellular crystal formation in *C. matruchotii*. Through detailed characterization of the calcified cells, we aimed to provide new insights into the mechanism and regulation of bacterial calcification involved in dental calculus formation.

Materials and methods

Bacterial strain and media

C. matruchotii (JCM9386) was cultured aerobically at 37 °C for 4 years in 25 mL of calcium-containing Ca (+) or calcium-free Ca (-) medium in 50 mL centrifuge tubes (T2318, Greiner Bio-one GmbH, Frickenhausen, Germany). The Ca (+) and Ca (-) media were prepared based on the formulation described by Ennever[13]. The Ca (+) medium contained following components per liter of 0.1 M N-tris (hydroxymethyl) methyl-2-aminoethanesulfonic acid (pH 7.4): glucose, 2 g; casein hydrate, 4 g; $NaHCO_3$, 1.85 g; $NaHPO_4{\cdot}2H_2O$, 550 mg; $CH_3COONa{\cdot}3H_2O$, 147 mg; $CaCl_2{\cdot}2H_2O$, 145 mg; $MgSO_4{\cdot}7H_2O$, 35 mg; $FeSO_4{\cdot}7H_2O$, 4 mg; $MnSO_4{\cdot}H_2O$, 0.15 mg; $NaMoO_4{\cdot}2H_2O$, 0.15 mg; para-aminobenzoic acid, 2 mg; riboflavin, 2 mg; calcium pantothenate, 2 mg; inositol, 2 mg; thiamine, 2 mg; nicotinic acid, 1 mg; pyridoxine HCl, 1 mg; biotin, 0.1 mg; folic acid, 0.1 mg; pimelic acid, 0.1 mg; thioctic acid, 0.1 mg; adenine, 20 mg; guanine, 20 mg; thymine, 20 mg; uracil, 20 mg; xanthine, 20 mg. The Ca (-) medium was identical to the Ca (+) medium, except that $CaCl_2{\cdot}2H_2O$ was omitted. Both media were supplemented with silica nano powder (average particle size: 12 nm) to serve as nucleation sites for calcification. The tubes were sealed and stored in an incubator at 37 °C for 4 years without changing or adding flesh medium.

Scanning electron microscopy (SEM)

Samples were fixed with 2.5% glutaraldehyde and placed in small envelopes made from No. 5 filter paper containing 3 mm square glass pieces. The samples were rinsed with distilled water, dehydrated through an acetone series, and then immersed in *t*-butyl alcohol. Subsequently, they were freeze-dried using a VFD-30 freeze dryer (VACUUM DEVICE Inc., Ibaraki, Japan). The glass pieces were coated with osmium using a HPC-30W plasma coater (VACUUM DEVICE Inc., Ibaraki, Japan) and observed by SEM (Regulus 8100, Hitachi, Japan).

Transmission electron microscopy (TEM)

Samples were pre-fixed in 2.5% glutaraldehyde overnight at 4 °C, washed, and suspended in 0.1 M phosphate buffer (pH 7.2), followed by post-fixation with 1% OsO_4. The samples were then embedded in 1% agar, cut into small cubes, dehydrated through a graded alcohol series (50% to 100%), and subsequently immersed in acetone. Infiltration was carried out by incubating the samples overnight in a 10:1 mixture of acetone and Epon 812 resin. The samples were then embedded in fresh Epon 812 resin. Ultra-thin sections were prepared and mounted on copper grids. The sections were stained with uranyl acetate and lead citrate, and observed using a TEM (JEM-1400 Plus, JEOL Ltd., Tokyo, Japan).

Elemental analysis

Elemental analysis and elemental mapping were performed using energy-dispersive X-ray spectrometer (EDX). Both osmium-fixed and osmium-free fixation protocols were employed. Samples were fixed with 2.5% glutaraldehyde and mounted on glass slides using cytospin method (SAKURA Finetek Japan Co., Ltd. Tokyo, Japan). The slides were washed with phosphate buffer, dehydrated through a graded alcohol series (50% to 100%), and immersed in acetone. The samples were then embedded in Epon 812 resin in an inverted orientation and ultra-thin sections were prepared. Some sections were stained with uranium, while others were left unstained. All sections were mounted on cupper grids and carbon-coated for reinforcement using VC-100 carbon coater (VACUUM DEVICE Inc., Ibaraki, Japan). Elemental analysis and mapping, including the detection of calcium, phosphorus, and silicon, were conducted using EDX equipped with a Dry SD30GV Detector (EX-14210M4G2T).

Statistical analysis

Statistical analyses were performed using Prism 9 (GraphPad Software, La Jolla, CA, USA). Two-tailed unpaired Student's t-test were applied, and a p-value < 0.05 was considered statistically significant ($^{*}p < 0.05$, $^{**}p < 0.01$, and $^{***}p < 0.001$). Results are expressed as mean ± SD, and all data points represent biological replicates.

Result

Calcium ions influence *C. matruchotii's* morphology and intercellular organization

Differences in bacterial phenotypes caused by calcium ions were observed by SEM. Under the Ca (-) condition, although the bacterial surface appeared smooth, rupture of the lipid bilayer and the formation of holes in the bacterial body were observed (Fig. 1A). In addition, intracellular contents were found to be leaking through these holes (Fig. 1B). In contrast, under the Ca (+) condition, both the length and width of *C. matruchotii* were significantly reduced, with the length in particular being decreased to less than half that of non-calcified bacteria (Fig. 1D). Moreover, calcified bacteria exhibited a less smooth morphology and showed a greater tendency to flocculate compared with those under the Ca (-) condition (Fig. 1E, F). *C. matruchotii* in the Ca (+) condition

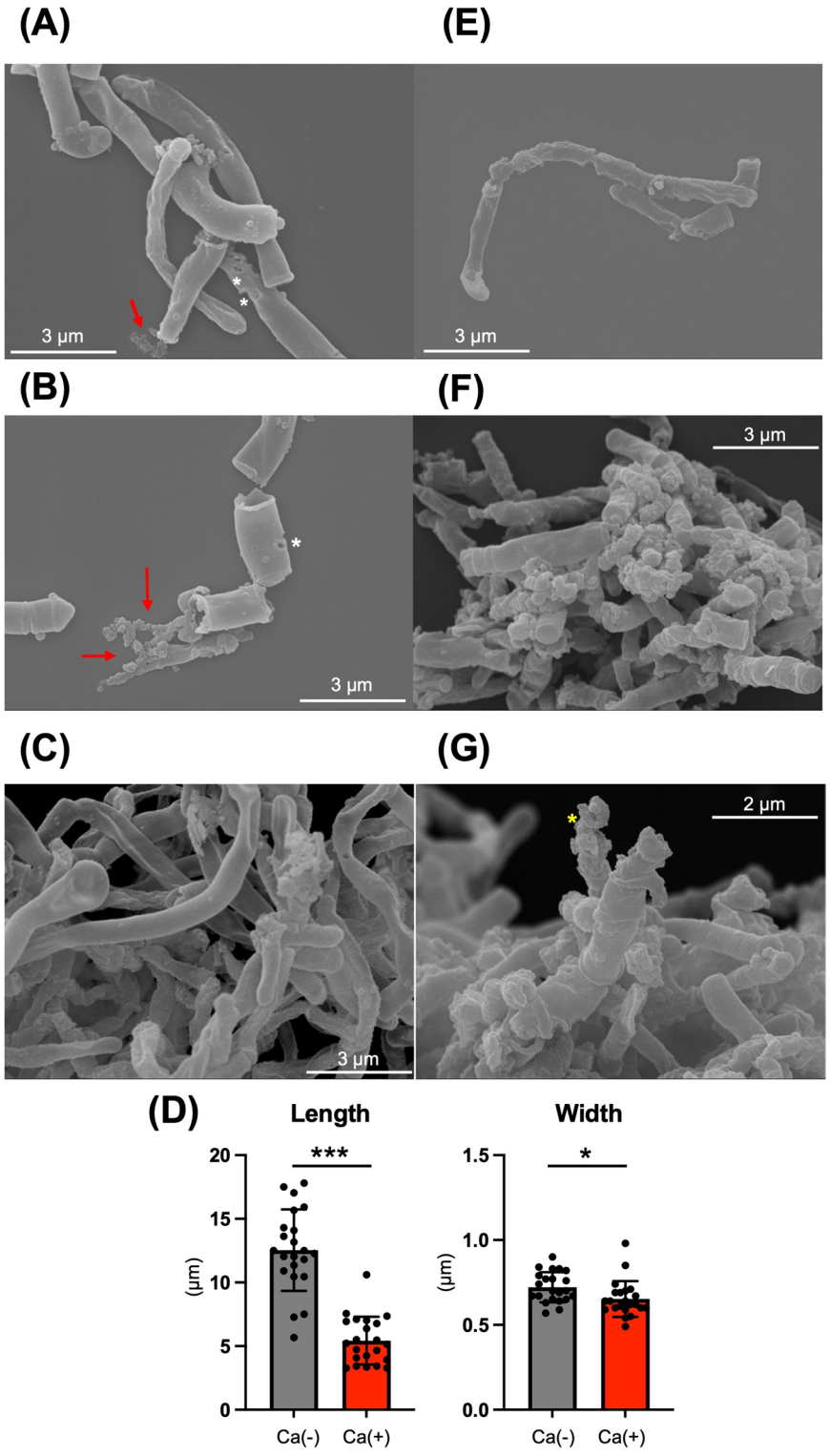

Fig. 1. SEM images of *C. matruchotii* under Ca (+) and Ca (-) conditions. (**A**) *C. matruchotii* under the Ca (-) condition. Red arrow indicates leakage of intracellular contents; white arrow indicates a hole in the bacterial membrane. (**B**) *C. matruchotii* under the Ca (-) condition. Red arrows indicate leakage of intracellular contents; white asterisk indicates a hole in the bacterial membrane. (**C**) Aggregated *C. matruchotii* under the Ca (-) condition. (**D**) Quantification of bacterial length and width under Ca (-) and Ca (+) conditions. (**E**) *C. matruchotii* under the Ca (+) condition. The bacterial surface appears wrinkled and shrunken compared to the Ca (-) condition. (**F**) Aggregated *C. matruchotii* under the Ca (+) condition. (**G**) High-magnification image of *C. matruchotii* under the Ca (+) condition showing fine, cauliflower-like surface structures.

exhibited a wrinkled surface, without observable holes, and no leakage of intracellular contents was observed (Fig. 1E). Higher magnification images revealed that the wrinkle-like structures were composed of finely raised, cauliflower-like structures (Fig. 1G). The intercellular gaps among *C. matruchotii* were reduced under the Ca (+) condition compared to the Ca (-) condition (Fig. 1C, E). These results suggest that calcium ions influence *C. matruchotii*'s morphology and intercellular organization.

Calcium ions play a critical role in facilitating the initiation of calcification

To further investigate intracellular changes, *C. matruchotii* under both Ca (+) and Ca (-) conditions was observed using TEM. Under the Ca (-) condition, no crystal formation was observed in *C. matruchotii.* Instead, rupture of the bacterial body and leakage of intracellular contents were noted, as observed by SEM (Fig. 2A). In contrast, under the Ca (+) condition, *C. matruchotii* remained structurally intact, and most cells showed low electron transmission, suggesting a low density of intracellular contents. Some cells also exhibited crystal formation (Fig. 2B). Higher magnification images revealed that under the Ca (-) condition, variations in electron transmission were present among individual cells. Although sparsely distributed regions of low transmission were observed, no crystals were detected (Fig. 2C). Cross-sectional images revealed that intracellular contents remained localized in the center of the cells, with no signs of crystal formation (Fig. 2D). In contrast, under the Ca (+) condition associated with calcification, amorphous regions of low electron transmission were observed throughout the cytoplasm. These amorphous regions were particularly prominent around the cell wall, where calcification appear to occur. Notably, crystals were always surrounded by amorphous material, and no isolated crystals were observed. (Fig. 2E, F). These results suggest that calcium ions play a critical role in maintaining *C. matruchotii*'s cell integrity and facilitating the initiation of calcification, potentially by inducing the accumulation of amorphous calcium phosphate-like material within and around bacterial cells.

The elemental analysis and mapping of crystals and amorphous-like structures in bacterial body of *C. matruchotii*

To confirm that the crystals observed by TEM represented calcification, elemental analysis was performed. EDX revealed that the intracellular, low electron-transmission regions corresponding to crystalline and amorphous-like structures observed in *C. matruchotii* under the Ca (+) condition were composed of calcium and phosphorus ions (Fig. 3A, i and ii). In contrast, the sparse low electron-transmission regions observed under the Ca (-) condition did not show characteristic X-ray peaks for calcium or phosphate ions (Fig. 3B, iii and iv). This result was further confirmed under the no-osmium fixation condition (Fig. S1).

Elemental mapping revealed that the calcium ions were not detected in non-calcifying microorganisms, and no accumulation of silicon was observed (Fig. 4A, B, D). Phosphate ions were consistently detected along the cell membrane, even in regions lacking calcification (Fig. 4C). Strong calcium accumulation was observed in the low electron-transmission crystalline regions, whereas weaker calcium accumulation was also detected in the low electron-transmission amorphous regions within the cell and around the cell membrane (Fig. 4D).

These findings suggest that calcification occurs specifically under the Ca (+) condition, while the structures observed under the Ca (-) condition are unrelated to calcium phosphate deposition.

Discussion

Dental calculus is composed of calcium phosphate crystals and bacteria. *C. matruchotii* is the most representative bacterium associated with dental calculus. Previous research on bacterial calcification has primarily focused on the composition of calcified material, more recent studies have begun to investigate the process of calcification itself[17,21].

Silicon has attracted attention as a potential nucleation factor for calcification, and previous studies have investigated its role in the calcification of *C. matruchotii*, together with silicon metabolism and the determination of its optimal concentration[20]. Based on these studies, which indicated that the addition of 0.01 mM SiO_2 was most favorable for calcification, we conducted our experiments using this SiO_2 concentration. Furthermore, since a decrease in silicon concentration over time has been observed, no specific accumulation of silicon was detected within the cells in our long-term calcified samples (Fig. 4).

Phosphate and its relationship with calcification have been extensively studied in both eukaryotic and prokaryotic organisms[22,23]. Polyphosphate was previously considered an inhibitor of calcification[24]. However, in marine bacteria and diatoms, it has been reported that inorganic phosphate can be stored as amorphous polyphosphate granules, which may release phosphate in response to environmental changes, potentially triggering the nucleation of phosphate minerals[22].

In humans, polyphosphate has been shown to induce alkaline phosphatase (ALP) expression[25], and this enzyme has been suggested to contribute to hydroxyapatite crystal formation[23,26]. In microbial calcification studies, *Escherichia coli*—alongside *C. matruchotii*—is a well-studied model organism. In *E. coli*, overexpression of alkaline phosphatase (PHO A) has been reported to enhance calcification[27]. Furthermore, *in vitro* experiments under phosphate-rich conditions showed that, even when phosphoproteins were present at concentrations sufficient to induce precipitation in solution, no crystallization occurred in viable bacteria[17]. This suggests that extracellular phosphate alone may not be a strong driving force for calcification in viable bacteria.

In *C. matruchotii*, elemental mapping revealed that regions with high phosphorus content did not always correspond to sites of calcification (Fig. 4A, C). Therefore, when these findings considered together with previous results in *E. coli*, it can be inferred that an excess of phosphate does not necessarily promote calcification. Then, the *C. matruchotii* also possesses alkaline phosphatase related to phosphate-based calcification, similar to *E.coli*[28]. Moreover, *C. matruchotii* has been reported to take up soluble phosphate (orthophosphate, Pi) and accumulate it as polyphosphate (polyP), similar to marine microorganisms[29]. Given the above, phosphate-rich conditions may not necessarily promote intracellular calcification in *C. matruchotii*. Rather, it is possible that soluble phosphate

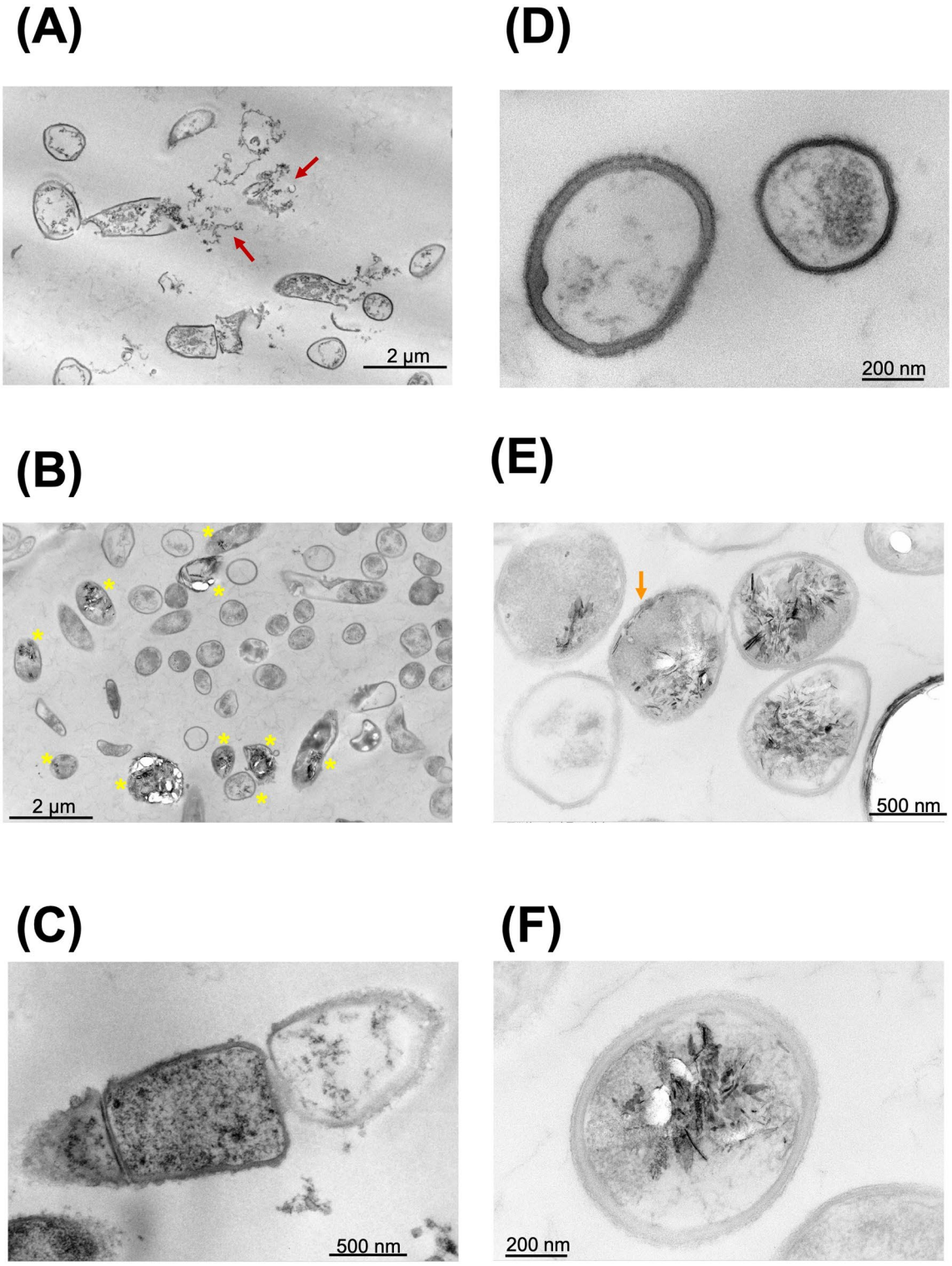

Fig. 2. TEM images of *C. matruchotii* under Ca (+) and Ca (-) conditions. (**A**) *C. matruchotii* under the Ca (-) condition. Red arrows indicate leakage of intracellular contents. (**B**) *C. matruchotii* under the Ca (+) condition. Most bacteria show amorphous structures. Yellow arrows indicate crystal formation within the bacterial body. (**C**) *C. matruchotii* under the Ca (-) condition at 20000x magnification. One cell shows low overall electron transmission, while another shows high transmission. No crystals are observed within the bacteria. (**D**) *C. matruchotii* under the Ca (-) condition at 40000x magnification showing no evidence of crystal formation. (**E**) *C. matruchotii* under the Ca (+) condition. Plate-like and needle-like crystals are visible inside the bacteria. Orange arrow indicates a crystal located along the cell wall. (**F**) *C. matruchotii* under the Ca (+) condition at 40000x magnification showing both crystals and amorphous structures within the bacterial body.

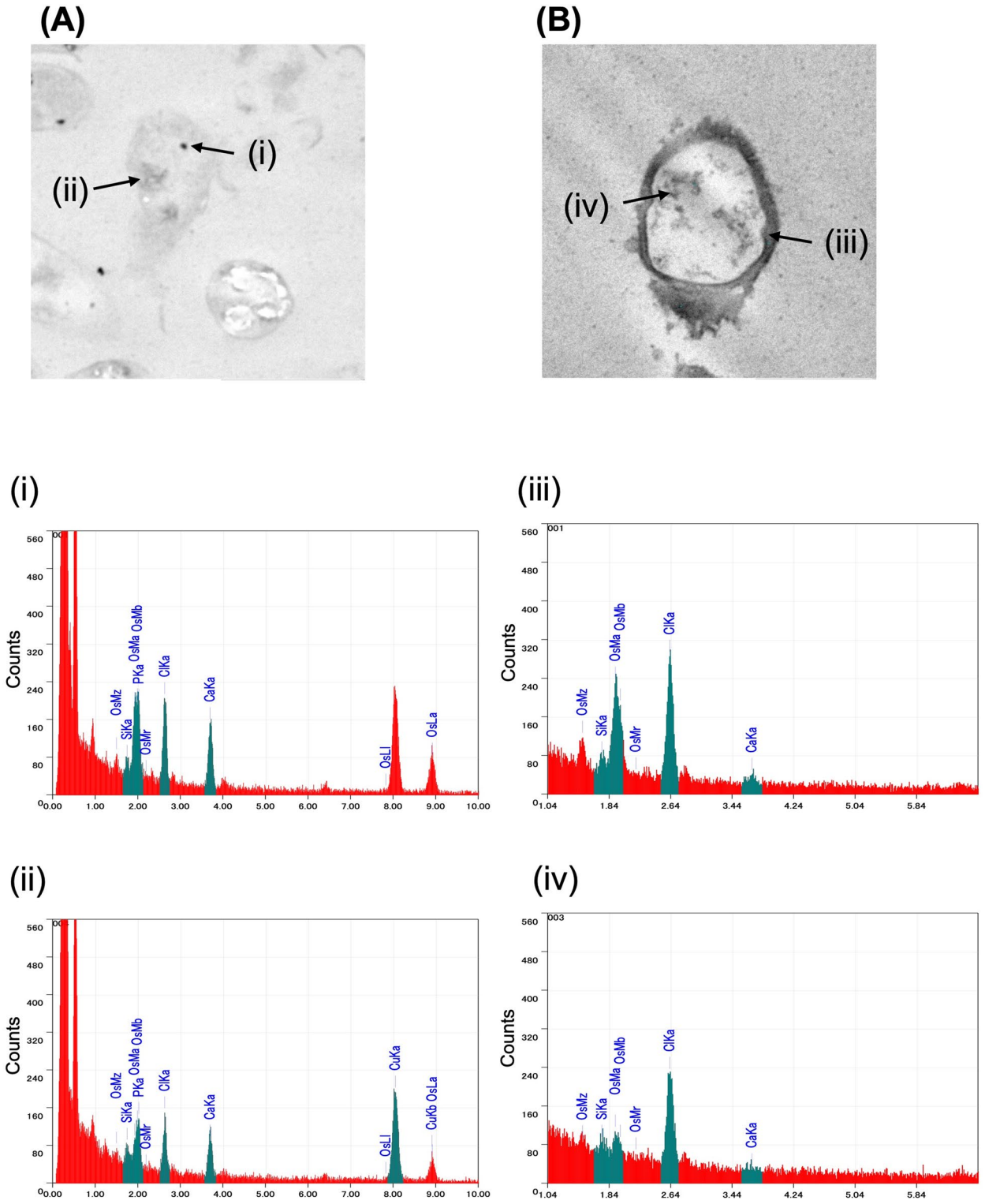

Fig. 3. TEM and EDX analysis of *C. matruchotii* under Ca (+) and Ca (-) conditions. (**A**) TEM image of *C. matruchotii* under the Ca (+) condition. EDX was performed at the regions marked (i) and (ii). (i) EDX spectrum obtained at the tip of the black arrow (i) in panel (**A**). (ii) EDX spectrum obtained at the tip of the black arrow (ii) in panel (**A**). (**B**) TEM image of *C. matruchotii* under the Ca (-) condition. EDX was performed the regions marked (iii) and (iv). (iii) EDX spectrum obtained at the tip of the black arrow (iii) in panel (**B**). (iv) EDX spectrum obtained at the tip of the black arrow (iv) in panel (**B**).

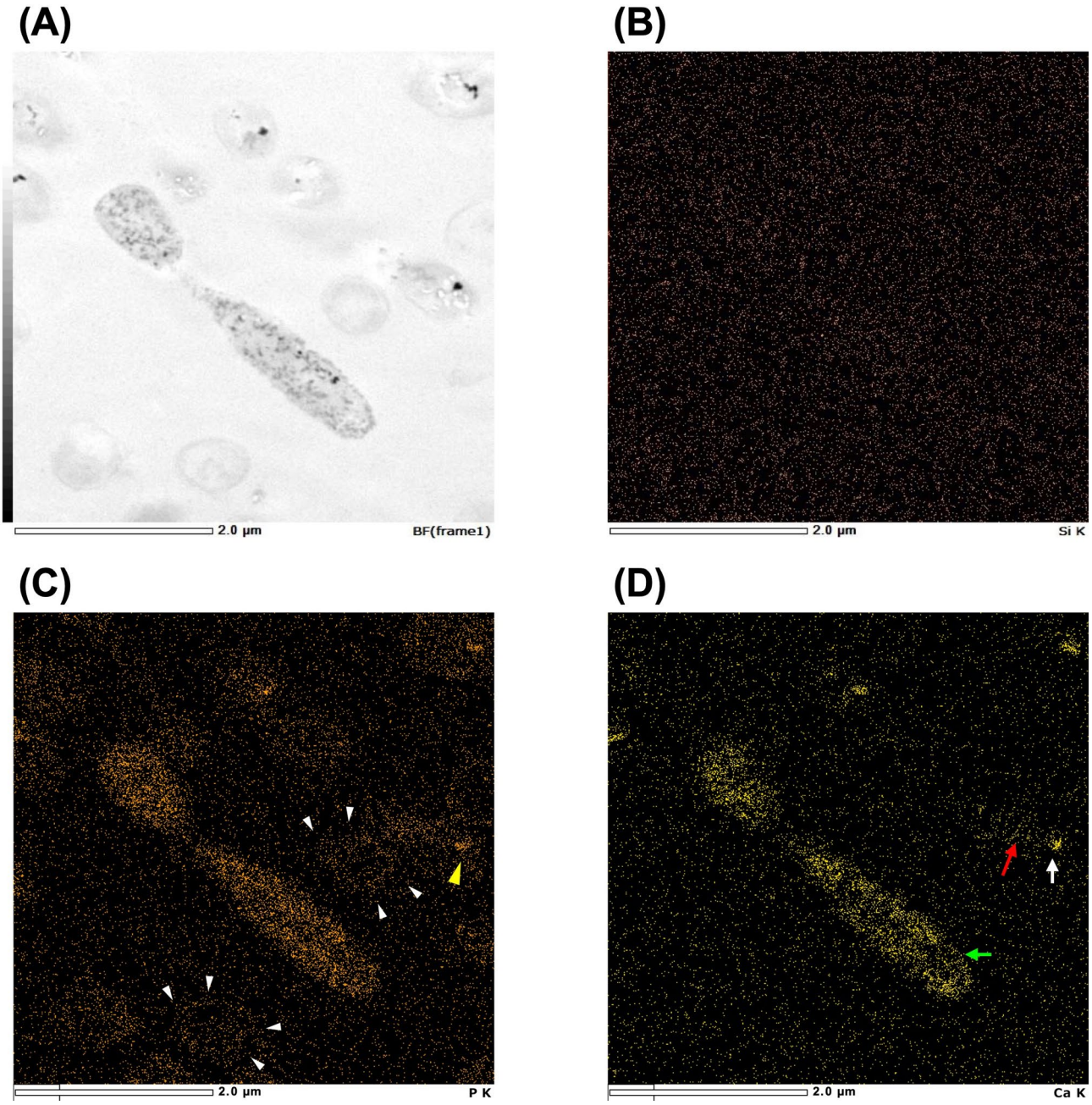

Fig. 4. TEM and element mapping analysis of *C. matruchotii* under Ca (+) conditions. (**A**) TEM image of *C. matruchotii* under the Ca (+) condition. (**B**) Elemental mapping of silicon. No silicon accumulation was observed within the field of view. (**C**) Element mapping of phosphorus. Phosphorus accumulation outlining the cell membrane is indicated by the white arrowhead. Strong phosphorus accumulation (yellow arrowhead) was observed in the low electron-transmission (crystalline) regions in TEM. (**D**) Elemental mapping of calcium. Calcium accumulation was observed only in *C. matruchotii* exhibiting intracellular calcification. Strong calcium accumulation was observed in the low electron-transmission (crystalline) regions (white arrow). Weak calcium accumulation was also detected in the low electron-transmission (amorphous) regions within the cell (red arrow) and around the cell membrane (green arrow).

(Pi) is taken up and stored as polyphosphate (polyP), which is then hydrolyzed back into orthophosphate by alkaline phosphatase under certain environmental conditions to facilitate calcification.

In this study, we focused on calcium ions, which have received relatively little attention to date, and aimed to further explore the role of extracellular calcium ions.

To minimize the influence of nucleation factors and exposure time – both of which are critical in crystal formation – and to focus solely on the presence and absence of calcium, we added 0.01mM silicon as a nucleation source and conducted calcification experiments over four years, a duration longer than that used in a previous

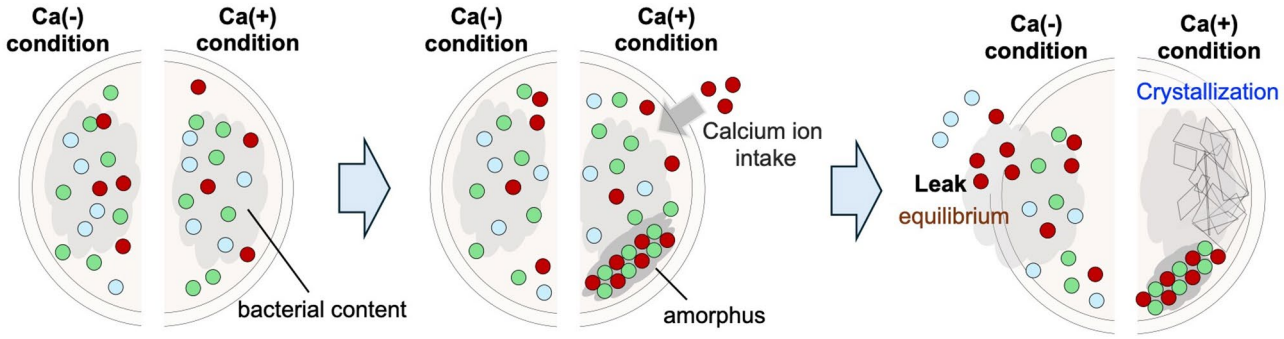

Fig. 5. Schematic illustration of intracellular calcification in response to calcium concentration differences. Green spheres: phosphate ions, red spheres: calcium ions. Initially, calcium ions and phosphate ions are present inside the cell. When the extracellular calcium ion concentration increases, an amorphous structure forms around the cell wall. This amorphous creates layer acts as a scaffold for subsequent in tricellular calcification. As more calcium ions are taken up from the extracellular environment, intracellular calcification progresses, leading to crystallization. In contrast, under low extracellular calcium conditions, pores form in the cell wall, causing leakage of cellular contents. The resulting interaction between the extracellular and intracellular environments leads to a further decrease in intracellular calcium concentration, thereby inhibiting calcification.

study[20]. Under the Ca (-) condition, no crystal formation was observed, while under the Ca (+) condition, crystals containing calcium and phosphate ions were detected. These results suggest that bacterial calcification is regulated by calcium ion.

Various factors, such as salt solubility and environmental conditions, influence crystallization and crystal growth, including calcification. In particular, the oral cavity experiences wide temperature fluctuations – from 0 °C to 90 °C – and pH shifts ranging from slightly alkaline to acidic. When focusing on bacterial structure, non-calcified bacteria showed ruptures and leakage of intracellular contents, whereas calcified bacteria maintained an intact lipid bilayer, showed no surface holes, and retained their intracellular contents (Figs. 1 and 2). Therefore, calcification of bacteria may help maintain structural integrity, making them less susceptible to environmental stress.

Under the Ca (-) condition, ion concentrations inside bacteria equilibrate with the external medium due to leakage, whereas in the Ca (+) condition, calcium ions are retained intracellularly due to the absence of leakage, thereby creating favorable environment for crystallization (Fig. 5). Inside calcified bacteria, TEM images showed amorphous, low-electron-transmission structures around the cell wall. Additionally, calcified bacteria were shorter in length compared to non-calcified bacteria. These amorphous structures were localized around the cell wall, and some bacteria showed crystal formation internally. This suggests that insoluble salts composed of calcium, phosphate, and possibly other ions may be trapped by membrane-associated proteins and lipids, forming amorphous aggregates. These structures may not only act as reservoirs for calcium ions but also reinforce the cell membrane after bacterial death, preventing rupture of the cell body.

Taken together, these findings suggest that *C. matruchotii* initially takes up calcium ions from the extracellular environment (e.g., saliva) and forms amorphous deposits around the inner cell wall. This may lead to a loss of cellular flexibility and inhibition of elongation or growth (Fig. 5). Eventually, calcifying *C. matruchotii* become shorter and tend to aggregate, potentially contributing to the nucleation of dental calculus by forming clusters of calcified bacterial components. This aggregation may also be advantageous under fluctuating environmental conditions of the oral cavity, as it helps shield the interior of the cluster from direct environment exposure.

Overall, our results suggest that the calcium ions play a key role in regulating the calcification of *C. matruchotii*, which is likely involved in the initial formation of dental calculus. Furthermore, the calcification process induces structural changes and aggregation in the bacteria themselves.

Under the measurement conditions employed in this study, dehydration was required during sample preparation due to inherent limitations of the method. Amorphous calcium phosphates are unstable to heat and dehydration[30,31]. Moreover, this measurement method cannot precisely determine the Ca: P ratio, making it impossible to accurately identify the state of amorphous calcium phosphates or the composition of the crystals. These issues are expected to be resolved in the future by combining cryo-fixation with cryo-electron microscopy and electron diffraction, techniques that have been advancing rapidly in recent years[32,33].

However, in the context of the actual oral cavity, the surrounding microbiome must also be considered. For example, *C. matruchotii* is thought to exist symbiotically with *Streptococcus sanguinis*, a catalase-positive bacterium that may act antagonistically toward acid-producing species such as *S. mutans*[34–36]. These microbial interactions may influence local pH, a critical factor in calcification. Since this study focuses solely on *C. matruchotii*, future investigation using co-culture systems or more complex models will be necessary to elucidate the detailed mechanisms of dental calculus formation.

Data availability

The datasets used and/or analyzed during the current study available from the corresponding author on reasonable request.

Received: 7 August 2025; Accepted: 30 December 2025
Published online: 06 January 2026

References

1. Levine, M. J., Tabak, L. A., Reddy, M. & Mandel, I. D. Nature of salivary pellicles in microbial adherence: role of salivary mucin. In: Mergenhagen SE (ed.). Molecular basis of oral microbial adhesion. *American Society of Microbiology*, 125–130 (1985).
2. Gibbons, R. J. Bacterial adhesion to oral tissues: a model for infectious diseases. *J. Dent. Res.* **68**, 750–760. https://doi.org/10.1177/00220345890680050101 (1989).
3. Marsh, P. D. Dental plaque as a microbial biofilm. *Caries Res.* **38**, 204–211. https://doi.org/10.1159/000077756 (2004).
4. Seneviratne, C. J., Zhang, C. F. & Samaranayake, L. P. Dental plaque biofilm in oral health and disease. *Chin. J. Dent. Res.* **14**, 87–94 (2011).
5. Schroeder, H. E. Formation and Inhibition of dental calculus. *J. Periodontol.* **40**, 643–646. https://doi.org/10.1902/jop.1969.40.11.643 (1969).
6. White, D. J. Dental calculus: recent insights into occurrence, formation, prevention, removal and oral health effects of supragingival and subgingival deposits. *Eur. J. Oral Sci.* **105**, 508–522. https://doi.org/10.1111/j.1600-0722.1997.tb00238.x (1997).
7. Darveau, R. P., Tanner, A. & Page, R. C. The microbial challenge in periodontitis. *Periodontol 2000.* **14**, 12–32. https://doi.org/10.1111/j.1600-0757.1997.tb00190.x (1997).
8. Akcali, A. & Lang, N. P. Dental calculus: the calcified biofilm and its role in disease development. *Periodontol 2000.* **76**, 109–115. https://doi.org/10.1111/prd.12151 (2018).
9. Rabbani, G. M., Ash, M. M. Jr. & Caffesse, R. G. The effectiveness of subgingival scaling and root planing in calculus removal. *J. Periodontol.* **52**, 119–123. https://doi.org/10.1902/jop.1981.52.3.119 (1981).
10. Cobb, C. M. Clinical significance of non-surgical periodontal therapy: an evidence-based perspective of scaling and root planing. *J. Clin. Periodontol.* **29** (Suppl 2), 6–16 (2002).
11. Eriksson, L., Lif Holgerson, P. & Johansson, I. Saliva and tooth biofilm bacterial microbiota in adolescents in a low caries community. *Sci. Rep.* **7**, 5861. https://doi.org/10.1038/s41598-017-06221-z (2017).
12. Esberg, A. et al. Corynebacterium matruchotii demography and adhesion determinants in the oral cavity of healthy individuals. *Microorganisms* **8** https://doi.org/10.3390/microorganisms8111780 (2020).
13. Ennever, J., Vogel, J. J. & Streckfuss, J. L. Synthetic medium for calcification of bacterionema matruchotii. *J. Dent. Res.* **50**, 1327–1330. https://doi.org/10.1177/00220345710500054101 (1971).
14. Takazoe, I. & Itoyama, T. Analytical electron microscopy of bacterionema matruchotii calcification. *J. Dent. Res.* **59**, 1090–1094. https://doi.org/10.1177/00220345800590062101 (1980).
15. Moorer, W. R., Cate, T., Buijs, J. F. & J. M. & Calcification of a cariogenic Streptococcus and of Corynebacterium (Bacterionema) matruchotii. *J. Dent. Res.* **72**, 1021–1026. https://doi.org/10.1177/00220345930720060501 (1993).
16. van Dijk, S. et al. Purification, amino acid sequence, and cDNA sequence of a novel calcium-precipitating proteolipid involved in calcification of Corynebacterium matruchotii. *Calcif Tissue Int.* **62**, 350–358. https://doi.org/10.1007/s002239900443 (1998).
17. Yoshikuni, Y. et al. Effect of phosphoproteins on intracellular calcification of bacteria. *Eur. J. Oral Sci.* **131**, e12929. https://doi.org/10.1111/eos.12929 (2023).
18. Sidaway, D. A. A Microbiological study of dental calculus. III. A comparison of the in vitro calcification of viable and non-viable microorganisms. *J. Periodontal Res.* **14**, 167–172. https://doi.org/10.1111/j.1600-0765.1979.tb00787.x (1979).
19. Souchay, A., Pouezat, J. A. & Menanteau, J. Mineralization of Streptococcus mutans in vitro. An ultrastructural study. *Oral Surg. Oral Med. Oral Pathol. Oral Radiol. Endod.* **79**, 311–320. https://doi.org/10.1016/s1079-2104(05)80225-2 (1995).
20. Linton, K. M. et al. A silicon cell cycle in a bacterial model of calcium phosphate mineralogenesis. *Micron* **44**, 419–432. https://doi.org/10.1016/j.micron.2012.09.008 (2013).
21. Li, Q., Zhou, F., Su, Z., Li, Y. & Li, J. Corynebacterium matruchotii: A confirmed calcifying bacterium with a potentially important role in the supragingival plaque. *Front. Microbiol.* **13**, 940643. https://doi.org/10.3389/fmicb.2022.940643 (2022).
22. Omelon, S., Ariganello, M., Bonucci, E., Grynpas, M. & Nanci, A. A review of phosphate mineral nucleation in biology and geobiology. *Calcif Tissue Int.* **93**, 382–396. https://doi.org/10.1007/s00223-013-9784-9 (2013).
23. Wang, Y. et al. Progress and applications of polyphosphate in bone and cartilage regeneration. *Biomed. Res. Int.* **2019** (5141204). https://doi.org/10.1155/2019/5141204 (2019).
24. Fleish, H. & Neuman, W. F. Mechanisms of calcification: role of collagen, polyphosphates, and phosphatase. *Am. J. Physiol.* **200**, 1296–1300. https://doi.org/10.1152/ajplegacy.1961.200.6.1296 (1961).
25. Muller, W. E. et al. Inorganic polymeric phosphate/polyphosphate as an inducer of alkaline phosphatase and a modulator of intracellular Ca2 + level in osteoblasts (SaOS-2 cells) in vitro. *Acta Biomater.* **7**, 2661–2671. https://doi.org/10.1016/j.actbio.2011.03.007 (2011).
26. Omelon, S., Georgiou, J., Variola, F. & Dean, M. N. Colocation and role of polyphosphates and alkaline phosphatase in apatite biomineralization of elasmobranch tesserae. *Acta Biomater.* **10**, 3899–3910. https://doi.org/10.1016/j.actbio.2014.06.008 (2014).
27. Cosmidis, J. et al. Calcium-Phosphate biomineralization induced by alkaline phosphatase activity in Escherichia coli: Localization, Kinetics, and potential signatures in the fossil record. *Front Earth Sci* **3**, 84. (2015).
28. Franker, C. K., McGee, M. P. & Rezzo, T. P. Alkaline phosphatase activity in a strain of bacterionema matruchotii. *J. Dent. Res.* **58**, 1705–1708. https://doi.org/10.1177/00220345790580071001 (1979).
29. Ghose, D. & Jones, R. S. Extracellular phosphate modulation and polyphosphate accumulation by Corynebacterium matruchotii and Streptococcus mutans. *Dent. J. (Basel).* **12** https://doi.org/10.3390/dj12110366 (2024).
30. Xie, B., Halter, T. J., Borah, B. M. & Nancollas, G. H. Tracking amorphous precursor formation and transformation during induction stages of nucleation. *Cryst. Growth Des.* **14**, 1659–1665. https://doi.org/10.1021/cg401777x (2014).
31. Meyer, J. L. & Eanes, E. D. A thermodynamic analysis of the amorphous to crystalline calcium phosphate transformation. *Calcif Tissue Res.* **25**, 59–68. https://doi.org/10.1007/BF02010752 (1978).
32. Lei, C. et al. Applications of cryogenic electron microscopy in biomineralization research. *J. Dent. Res.* **101**, 505–514. https://doi.org/10.1177/00220345211053814 (2022).
33. Wang, X., Yang, J., Andrei, C. M., Soleymani, L. & Grandfield, K. Biomineralization of calcium phosphate revealed by in situ liquid-phase electron microscopy. *Commun. Chem.* **1**, 80 (2018).
34. Richards, V. P. et al. Microbiomes of Site-Specific dental plaques from children with different caries status. *Infect. Immun.* **85** https://doi.org/10.1128/IAI.00106-17 (2017).
35. Mark Welch, J. L., Rossetti, B. J., Rieken, C. W., Dewhirst, F. E. & Borisy, G. G. Biogeography of a human oral Microbiome at the micron scale. *Proc. Natl. Acad. Sci. U S A.* **113**, E791–800. https://doi.org/10.1073/pnas.1522149113 (2016).
36. Kreth, J., Zhang, Y. & Herzberg, M. C. Streptococcal antagonism in oral biofilms: Streptococcus sanguinis and Streptococcus gordonii interference with Streptococcus mutans. *J. Bacteriol.* **190**, 4632–4640. https://doi.org/10.1128/JB.00276-08 (2008).

Acknowledgements
We thank Mr. Mitsuru Yokoyama for assistance with SEM and TEM data collection.

Author contributions
Naoko.O. and Naoya.O. conceived and designed the experiments, and Naoko.O., M.O., K.T., S.O. performed the experiments. Naoko.O., M.O. collected data, and Naoko.O., M.O., K.T., I.T., S.O., M.S., Naoya.O. analyzed the data. Naoko.O., M.O., K.T., I.T. wrote the paper. All authors reviewed the manuscript.

Funding
This work was supported by JSPS KAKENHI grants (grant numbers JP23K09459 [Naoko.O.], JP24K02614 [Naoya.O.], JP24K23551 [K.T.]).

Declarations

Competing interests
The authors declare no competing interests.

Additional information
Supplementary Information The online version contains supplementary material available at https://doi.org/10.1038/s41598-025-34628-6.

Correspondence and requests for materials should be addressed to N.O.

Reprints and permissions information is available at www.nature.com/reprints.

Publisher's note Springer Nature remains neutral with regard to jurisdictional claims in published maps and institutional affiliations.